Available online at www.sciencedirect.com

ScienceDirect

Procedia Engineering 79 (2014) 427 – 436

Procedia Engineering

www.elsevier.com/locate/procedia

37th National Conference on Theoretical and Applied Mechanics (37th NCTAM 2013) & The 1st International Conference on Mechanics (1st ICM)

Application of Uniform Design and Quantum-Behaved Particle Swarm Optimization in Solving the Sensitivity Problem a Railway Vehicle System

Cheng-Kang Lee[a], Yung-Chang Cheng[b,*]

[a]*Department of Industrial Engineering and Management, Cheng Shiu University, Kaohsiung 833, Taiwan*
[b]*Department of Mechanical and Automation Engineering, National Kaohsiung First University of Science and Technology, Kaohsiung, 811, Taiwan*

Abstract

This paper, based on uniform design and quantum-behaved particle swarm optimization (QPSO), aims to solve the sensitivity problem of a railway vehicle system with fourteen degrees of freedom and nonlinear coupled differential equations of motion. The vehicle is very sensitive to wheel conicity if suspension parameters are not designed properly. A new heuristic nonlinear creep model is applied and is determined by adding the linear creep moment and the semi-axis lengths in the nonlinearity of the saturation constant. The vehicle's critical hunting speed is determined by Lyapunov's indirect method. This paper has demonstrated that the integration of uniform design and quantum-behaved particle swarm optimization can effectively determine the optimal solutions for suspension parameters. After applying the optimization procedure presented in this paper, the vehicle's critical hunting speed can be no longer sensitive to wheel conicity.

Selection and peer-review under responsibility of the National Tsing Hua University, Department of Power Mechanical Engineering

Keywords: Uniform design, Quantum-behaved particle swarm optimization, New nonlinear creep model, Critical hunting speed.

Nomenclature

* Corresponding author. Tel.:+886-7-601-1000; fax:+886-7-601-1066.
E-mail address: yccheng@nkfust.edu.tw

Selection and peer-review under responsibility of the National Tsing Hua University, Department of Power Mechanical Engineering
doi:10.1016/j.proeng.2014.06.364

a	half of track gauge
$\bar{a}$, $\bar{b}$	semi-axis lengths
b_1	half of primary yaw spring arm and primary yaw damping arm
b_2	half of secondary longitudinal spring arm
b_3	half of secondary longitudinal damping arm
C_{ij}	creepage and spin coefficients
C_{px}, C_{py}	yaw and lateral damping of primary suspension
C_{sx}, C_{sy}	yaw and lateral damping of secondary suspension
f	coefficient of friction between wheels and rails
f_{11}	lateral creep force coefficient
f_{12}	lateral / spin creep force coefficient
f_{22}	spin creep force coefficient
f_{33}	longitudinal creep force coefficient
F_R	limiting resultant force for traditional nonlinear creep model
$F_R^{'}$	resultant creep force of the traditional nonlinear creep model
$F_R^{*'}$	resultant creep force of new nonlinear creep model
G	combined shear modulus of rigidity of wheel and rail materials
h_c	vertical distance from wheelset center of gravity to car body
h_T	vertical distance from wheelset center of gravity to secondary suspension
I_{cz}	yaw moment of inertia of car body
I_{tz}	yaw moment of inertia of truck frame
I_{wz}	yaw moment of inertia of wheelset
K_{px}, K_{py}	longitudinal and lateral stiffness of primary suspension
K_{sx}, K_{sy}	longitudinal and lateral stiffness of secondary suspension
L_1	half of primary lateral spring arm
L_2	half of primary lateral damping arm
L_c	longitudinal distance from wheelset center of gravity to car body
m_c	car body mass
m_t	truck frame mass
m_w	wheelset mass
M_{szc}	suspension moment acting in vertical direction on car body
M_{szij}	suspension moment acting in vertical direction on front and rear wheelsets
M_{szti}	suspension moment acting in vertical direction on front and rear truck frames
N	normal force acting on wheelset in equilibrium state
N^*	normal force between rails and wheels
r_0	nominal rolling radius of wheelset
R	radius of curvature of track
R_{st}	index for measuring robustness of vehicle system
U_{30}^*	uniform table
α_{ij}	saturation constant in nonlinear creep force model for front and rear wheelsets
β_{ij}	nonlinearity constant in nonlinear creep force model for front and rear wheelsets
ϕ_{se}	superelevation angle of curved track

1. Introduction

The high-speed railway (HSR) has already become one of the most important transportation systems in modern society. For studies on the dynamic stability of a vehicle running on curved tracks, a car is generally modeled by systems of various degrees of freedom with traditional linear and nonlinear creep model. Molatefi *et al*. [1] and Polach [2] investigated the dynamic responses and critical speeds of railway vehicle with both linear and nonlinear

creep models. Little attention has so far been given to the robustness of critical hunting speed. However, the sensitivity problem of critical hunting speed is noticeable.

Evaluation of a complex system's performance measure requires a lot of computation time if the performance measure is determined by the system's complex governing equations. An efficient approach to dealing with the optimization problem for a complex system is performing a series of computer experiments. In this study, uniform design is utilized to devise experiments with control factors of many levels. Uniform design has been widely used in the optimization processes for many engineering applications. Liang *et al*. [3] reported the applications of uniform design in chemistry and chemical engineering. According to the uniform design method, Peng *et al*. [4] presented a uniform-differential evolution algorithm to accelerate the convergence speed of differential evolution and improve the stability. Uniform design was employed by Yang *et al*. [5] to arrange the experimental scheme for optimizing formulation of friction materials.

Particle swarm optimization (PSO) is a kind of swarm intelligence methods and is usually employed to solve global optimization problems. Inspired by the social behavior of bird flocking and fish schooling, Kennedy and Eberhart [6] proposed the particle swarm optimization (PSO) method in 1995. The main disadvantage of PSO is that the global convergence cannot be guaranteed. PSO is not a global optimization algorithm (Van Den Bergh and Engelbrecht [7]). To address this problem, Sun *et al*. [8, 9] introduced the quantum theory into PSO and proposed a quantum-behaved particle swarm optimization (QPSO) algorithm, which is a global convergence guaranteed method. The experimental results reported in [8, 9] show that QPSO works better than standard PSO on some widely applied benchmark functions.

This paper aims to apply uniform design and quantum-behaved particle swarm optimization to increase the robustness of a railway vehicle which has fourteen nonlinear equations of motion and fourteen degrees of freedom. The novel nonlinear creep model presented by Cheng [10] is adopted as the nonlinear creep model for the vehicle. The noise factor for the vehicle is wheel conicity whereas the control factors are suspension parameters. To advance the robustness for the vehicle, quantum particle swarm optimization is used. To let initial particles spread uniformly in the design space, uniform design is used. After iterations of quantum particle swarm algorism, the optimization solution for the 14-DOF vehicle system will be obtained.

2. New Nonlinear Creep Model

Considering the effect of the vehicle speed on the creep coefficients, the new nonlinear creep model is constructed and presented by modifying the traditional heuristic nonlinear creep model. The detailed descriptions are presented as follows.

(1). Calculate the creep coefficients

According to the Kalker's linear theory (Garg and Dukkipati [11]), the creep coefficients are given as

$$f_{11} = \left(\bar{a}\bar{b}\right) GC_{22},\ f_{12} = \left(\bar{a}\bar{b}\right)^{3/2} GC_{23},\ f_{22} = \left(\bar{a}\bar{b}\right)^{2} GC_{33},\ f_{33} = \left(\bar{a}\bar{b}\right) GC_{11} \tag{1}$$

where G is the combined shear modulus of rigidity of wheel and rail materials and given by Garg and Dukkipati [11]. C_{11}, C_{22}, C_{23} and C_{33} are creepage and spin coefficients given by Cheng [10]. $\bar{a}$ and $\bar{b}$, are the semi axes lengths at the contact area between rails and wheels presented in Appendix. Therefore, the Equation (1), the creep coefficients, f_{ij}, of the new nonlinear creep model are functions of vehicle speed V.

(2). Calculation of the semi axes lengths of the contact area between rails and wheels

Following Hertz contact theory, the shape of contact areas between rails and wheels is assumed to be elliptical. According to the notation used by Garg and Dukkipati [11], the semi axes lengths, $\bar{a}$ and $\bar{b}$ are given by

$$\bar{a} = m\left[\frac{3\pi N^{*}\left(K_1 + K_2\right)}{4K_3}\right]^{1/3},\ \bar{b} = n\left[\frac{3\pi N^{*}\left(K_1 + K_2\right)}{4K_3}\right]^{1/3} \tag{2}$$

where N^{*} is the normal force between rails and wheels. In this paper, assuming static force equilibrium in the vertical direction, the normal force N^{*} is equal to N_{Lz} and N_{Rz} given by Cheng [10]. Therefore, the semi axes

lengths, $\bar{a}$ and $\bar{b}$ vary with railway vehicle speeds. $K_1 \sim K_3$ are given by Cheng [10].

The coefficients, m and n, are given by Garg and Dukkipati [11]. By using the curve fitting technique in the curve fitting toolbox of MATLAB software, m and n can be shown in terms of θ and given by

$$m = 37.44\theta^{-0.7236} - 0.451 \tag{3a}$$

$$n = \frac{6.868\times10^{-5}\theta^5 - 0.0008207\theta^4 + 0.8561\theta^3 + 6.708\theta^2 - 2.288\theta - 0.5623}{\theta^3 + 37.27\theta^2 + 13.11\theta - 15.28} \tag{3b}$$

where θ is defined and given by Garg and Dukkipati [11].

(3).Calculate the nonlinear creep forces and moments.

According to Garg and Dukkipati [11], the normalized longitudinal and lateral creep forces and the spin creep moment are calculated as

$$F^*_{kxijN} = \frac{F^*_{kxij}}{fN},\ F^*_{kyijN} = \frac{F^*_{kyij}}{fN},\ M^*_{kzijN} = \frac{M^*_{kzij}}{CfN} \tag{4}$$

where subscripts $k = L, R$ indicate that the corresponding properties related to the left and right wheels, respectively. C is given by (Garg and Dukkipati [11])

$$C = \sqrt{\bar{a}\bar{b}} \tag{5}$$

Considering the spin creep moment, by following the approach of heuristic nonlinear creep model, the nonlinearity β^*_{kij} of the saturation constant for the new nonlinear creep model is given by

$$\beta^*_{kij} = \frac{\sqrt{\left(F^*_{kxij}\right)^2 + \left(F^*_{kyij}\right)^2 + \left(M^*_{kzij}/C\right)^2}}{fN} \tag{6}$$

where F^*_{kxij}, F^*_{kyij} and M^*_{kzij} indicate the linear creep forces and creep moments given by Cheng [10]. By following Horak and Wormley's approach [12], the saturation to the constant α_{ij} in the new nonlinear creep formalisms given as

$$\alpha_{ij} = \begin{cases} \dfrac{1}{\beta_{ij}}\left[\beta_{ij} - \dfrac{1}{3}\beta_{ij}^2 + \dfrac{1}{27}\beta_{ij}^3\right] & \text{for } \beta_{ij} \le 3 \\ \dfrac{1}{\beta_{ij}} & \text{for } \beta_{ij} \ge 3 \end{cases},\ \beta_{ij} = \frac{\beta_{Rij} + \beta_{Lij}}{2} \tag{7}$$

3. Equations of Motion of Railway Vehicle Model

Consider a railway vehicle travelling on a curved track with radius R (Figure 1). The governing equations of motion for lateral displacement y_{ti}, and yaw angle ψ_{ti} of the truck frame are given as

$$m_t\ddot{y}_{ti} = F_{syti} + (\frac{V^2}{gR} - \phi_{se})m_t g\ ,\ I_{tz}\ddot{\psi}_{ti} = M_{szti} \tag{8}$$

Meanwhile, the governing equations of motion for lateral displacement y_c, and yaw angle ψ_c of the car body are

$$m_c\ddot{y}_c = F_{syc} + (\frac{V^2}{gR} - \phi_{se})m_c g\ ,\ I_{cz}\ddot{\psi}_c = M_{szc} \tag{9}$$

where V is the speed of the railway vehicle in the forward direction and ϕ_{se} is the superelevation angle of curved tracks.

The governing coupled differential equations of motion for lateral displacement y_{wij}, and yaw angle ψ_{wij} of the wheelsets are

$$m_w\left(\ddot{y}_{wij}-\frac{V^2}{R}\right)=-\frac{2\alpha_{ij}f_{11}}{V}\left(\dot{y}_{wij}-V\psi_{wij}\right)-\frac{2\alpha_{ij}f_{12}}{V}\left(\dot{\psi}_{wij}-\frac{V}{R}\right)-\frac{2r_0\alpha_{ij}f_{11}}{V}\left(\frac{\lambda}{a}\right)\dot{y}_{wij}$$
$$-\left[\left(W_{ext}+m_wg\right)+\frac{V^2W_{ext}}{gR}\phi_{se}\right]\left(\frac{\lambda}{a}\right)y_{wij}-\left(W_{ext}+m_wg\right)\phi_{se}+\frac{V^2W_{ext}}{gR}+F_{syij} \tag{10}$$

$$I_{wz}\ddot{\psi}_{wij}=-\frac{2a\lambda\alpha_{ij}f_{33}}{r_o}y_{wij}+\frac{2\alpha_{ij}f_{12}}{V}\dot{y}_{wij}-\left(I_{wy}\frac{V}{r_o}-\frac{2r_o\alpha_{ij}f_{12}}{V}\right)\left(\frac{\lambda}{a}\right)\dot{y}_{wij}-2\alpha_{ij}f_{12}\psi_{wij}$$
$$+\left(W_{ext}+m_wg+\frac{V^2W_{ext}}{gR}\phi_{se}\right)a\lambda\psi_{wij}-\alpha_{ij}\left(\frac{2a^2f_{33}}{V}+\frac{2f_{22}}{V}\right)\dot{\psi}_{wij}+\frac{2\alpha_{ij}}{R}\left(a^2f_{33}+f_{22}\right) \tag{11}$$
$$+M_{szij}$$

where $\alpha_{ij}=\alpha_{ij}\left(y_{wij},\dot{y}_{wij},\psi_{wij},\dot{\psi}_{wij}\right)$ Note also that the physical quantities F_{syc}, F_{syti}, M_{szc}, M_{szti}, F_{syij}, and M_{szij} are suspension forces and moments and given in Cheng [10]. The 14-DOF model of the railway vehicle is therefore given by Equations (8)–(11).

4. Stability Analysis

4.1 Lyapunov indirect method

In this study, with the wheels having conical profiles, and the large radius and small elevation angle of curved tracks, the hunting motions of wheelsets will occur as a vehicle negotiates curved tracks. Hunting stability, especially critical hunting speeds of the linear and simple railway vehicle system evaluated using the Routh-Hurwitz criterion, has been widely investigated. In fact, the railway vehicle system has many complex nonlinear factors including nonlinear creep forces and moments, wheel conicity, flange contact forces and so on. In this study, the 14-DOF vehicle model is an autonomous system. Because the Lyapunov indirect method (Vidyasager [13]) can be employed for autonomous systems, the effects of various physical parameters on the critical hunting speed of the 14-DOF vehicle model can be analyzed with various wheel conicities.

Therefore, the 14-DOF nonlinear model for the railway vehicle given in Equations (8)-(11) can be re-expressed as the following system of first-order differential equations:

$$\dot{\mathbf{x}}(\mathbf{t})=\mathbf{f}\left[\mathbf{x}(\mathbf{t})\right] \tag{12}$$

where $\mathbf{x(t)}$ is a 28×1 vector of the state variables.

For any given vehicle velocity, V, the following determinant matrix can be defined:

$$\mathbf{A}=\left[\frac{\partial\mathbf{f(x)}}{\partial\mathbf{x}}\right]_{\mathbf{x}=\mathbf{x_0}} \tag{13}$$

where $\mathbf{x_0}$ is the equilibrium point and satisfies $\mathbf{f}\left[f_0\right]=\mathbf{0}$. The dynamic system will be unstable if any one of the eigenvalues of matrix A has a positive real part. The maximum allowable velocity for which the eigenvalues of associated determinant matrix A has a non-positive real part is the critical hunting speed.

4.2 Hunting Stability Analysis

The effects of the system data parameters listed in Cheng [10] on critical hunting speeds for a railway vehicle are investigated. The type of bogie in the vehicle model is the freight vehicle used by Ahmed and Sankar [14]. Meanwhile, the tread profile of the wheel employed in the calculation of critical hunting speeds is assumed to be perfectly conical.

Fig. 2 presents the effect of the longitudinal stiffness K_{px} of primary suspension on the critical hunting speeds with various wheel conicities. The critical hunting speed increases with increasing K_{px}. Meanwhile, the critical hunting speeds evaluated with wheel conicity of 0.05 are greater than those obtained with wheel conicities of 0.07 and 0.09. However, the critical hunting speeds evaluated with wheel conicity of 0.07 exceed than those obtained

with wheel conicity of 0.05 as K_{px} is higher than 1.5×10^6 N/m.

Fig. 3 illustrates the effects of lateral damping C_{sy} of secondary suspension on critical hunting speeds with various wheel conicities. The critical hunting speed increases as C_{sy} increases. Moreover, the critical hunting speeds evaluated from the wheel conicities of 0.05 are greater than those evaluated using the wheel conicities of 0.07 and 0.09.

5. Optimization

5.1 Uniform design

Uniform design, proposed by professor Fang and Wang [15], is a kind of space filling design. Uniform design can be used to construct a set of experimental points which are scattered uniformly in a continuous design space. For a particle swarm optimization, the initial population of particles is determined randomly. Therefore, the initial population of particles might not be distributed uniformly in the design space. For this reason, this paper adopts uniform design to plan a set of experimental points and regards the experimental points as the initial population of particles before executing the subsequent quantum-behaved particle swarm optimization. For the vehicle system considered in this paper, 6 suspension parameters, K_{px}, K_{py}, K_{sx}, K_{sy}, C_{sx} and C_{sy}, are considered as control factors. Moreover, the number of particles is specified as 30. Thus, the uniform table $U^*_{30}(30^6)$ is chosen to construct the 30 particles of initial population. Table 1 shows the upper and lower bounds of suspension parameters. Table 2 shows the uniform table $U^*_{30}(30^6)$, where the integers represent the levels of parameters. To apply the uniform table $U^*_{30}(30^6)$, every suspension parameter must be divided into 30 levels between the parameter's upper and lower bounds. For each experiment, on the basis of Lyapunov's indirect method [13], critical hunting speed is evaluated three times under three different wheel conicites, λ=0.05, λ=0.07, and λ=0.09. The index for measuring robustness of the vehicle system is defined here by

$$R_{st} = 100\times\frac{STD(V_1,V_2,V_3)+1}{AVG(V_1,V_2,V_3)} \tag{14}$$

where $STD(V_1,V_2,V_3)$ and $AVG(V_1,V_2,V_3)$ denote respectively the standard deviation and the average of speeds V_1, V_2, and V_3. When the index R_{st} is decreased, critical hunting speeds can be advanced and sensitivity of speeds can be compressed. The lower the R_{st} is, the higher the robustness is. Table 3 shows the results of experiments, where the best solution occurs at the 30th experiment.

5.2 Quantum-behaved particle swarm optimization

The QPSO algorithm has been applied to successfully solve a wide range of continuous optimization problems. Here, we also apply QPSO to search for the optimal solutions of suspension parameters. For the QPSO implemented here, the number of particles is 30 and linearly decreasing contraction-expansion coefficient strategy is used. The 30 experiments presented in the section 4.1 are regarded as the initial population of particles. The convergence history of the index R is shown in Figure 2, where the value of R is decreased from 1.51 to 0.22. Table 4 shows the optimal solutions for suspension parameters. Finally, the original critical hunting speeds, the best critical hunting speeds obtained from uniform table, and the optimized critical hunting speeds evaluated by the QPSO algorithm are presented in Table 5. After optimization, the critical hunting speeds under three different wheel conicities become the same, which means the critical hunting speed is no more sensitive to the noise factor, wheel conicity. Robustness of the vehicle system is increased successfully.

6. Conclusion

A new nonlinear creep model has been constructed and utilized to analyze the hunting stability of a high-speed railway vehicle during curving. The dynamics of the railway vehicle has been fully described utilizing a 14-DOF model. The suspension parameters of the vehicle system have been optimized. The optimization process is

composed of two phases. The first phase is to execute a set of experiments planned by uniform design method. The second phase is to apply quantum-behaved particle swarm optimization to search for the optimal solutions for suspension parameters. After optimization, the vehicle's critical hunting speeds under three different wheel conicities have become totally the same value and equal to 457km/hr. This paper has shown that the integration of uniform design and quantum-behaved particle swarm optimization is a good strategy for advancing the robustness of a railway vehicle system.

Acknowledgements

The authors gratefully acknowledge the financial support provided for this study by the National Science Council of Taiwan, R. O. C., under Grant no. NSC 101-2221-E-327-033.

Table 1. Lower and upper bounds for suspension parameters

Suspension parameter	K_{px} (N/m)	K_{py} (N/m)	K_{sx} (N/m)	K_{sy} (N/m)	C_{sx} (N-s/m)	C_{sy} (N-s/m)
Lower bound	300000	300000	50000	50000	50000	50000
Basic value	980000	390000	350000	350000	320000	100000
Upper bound	2500000	2500000	2500000	2500000	1500000	1500000

Table 2. Uniform Table $U_{30}^{*}(30^{6})$

No. of Experiments	K_{px}	K_{py}	K_{sx}	K_{sy}	C_{sx}	C_{sy}
1	1	4	10	14	18	25
2	2	8	20	28	5	19
3	3	12	30	11	23	13
4	4	16	9	25	10	7
5	5	20	19	8	28	1
6	6	24	29	22	15	26
7	7	28	8	5	2	20
8	8	1	18	19	20	14
9	9	5	28	2	7	8
10	10	9	7	16	25	2
11	11	13	17	30	12	27
12	12	17	27	13	30	21
13	13	21	6	27	17	15
14	14	25	16	10	4	9
15	15	29	26	24	22	3
16	16	2	5	7	9	28
17	17	6	15	21	27	22

18	18	10	25	4	14	16
19	19	14	4	18	1	10
20	20	18	14	1	19	4
21	21	22	24	15	6	29
22	22	26	3	29	24	23
23	23	30	13	12	11	17
24	24	3	23	26	29	11
25	25	7	2	9	16	5
26	26	11	12	23	3	30
27	27	15	22	6	21	24
28	28	19	1	20	8	18
29	29	23	11	3	26	12
30	30	27	21	17	13	6

Table 3. Results of critical hunting speeds

No. of Experiments	V_1 (km/h) λ=0.05	V_2 (km/h) λ=0.07	V_3 (km/h) λ=0.09	R_{st}
1	94	86	78	10.47
2	111	283	89	66.60
3	133	116	103	13.67
4	148	129	112	14.66
5	345	339	291	9.41
6	176	152	130	15.73
7	168	145	125	15.42
8	208	326	288	22.35
9	202	366	321	28.93
10	415	353	332	12.04
11	214	196	149	18.55
12	316	236	170	30.79
13	332	467	191	42.12
14	227	314	192	26.12
15	538	453	437	11.61
16	198	288	139	36.50
17	484	449	376	12.86
18	284	300	328	7.65
19	198	188	149	15.08

20	573	496	450	12.47
21	484	465	453	3.56
22	351	516	492	19.90
23	370	293	464	23.06
24	366	300	437	18.91
25	497	466	447	5.58
26	222	527	174	62.55
27	315	474	459	21.34
28	550	295	516	30.74
29	299	358	509	28.12
30	479	471	467	1.51

Table 4. Optimal solutions for suspension parameters

Parameter	K_{px}(N/m)	K_{py}(N/m)	K_{sx}(N/m)	K_{sy}(N/m)	C_{sx}(N-s/m)	C_{sy}(N-s/m)
Optimal solution	2040723	1567538	2500000	1230013	1052827	1111631

Table 5. Results of critical hunting speeds after optimization

State	V_1 (km/h)	V_2 (km/h)	V_3 (km/h)	R_{st}
Original	333	316	308	13.77
After uniform design	479	471	467	1.51
After optimization	457	457	457	0.22

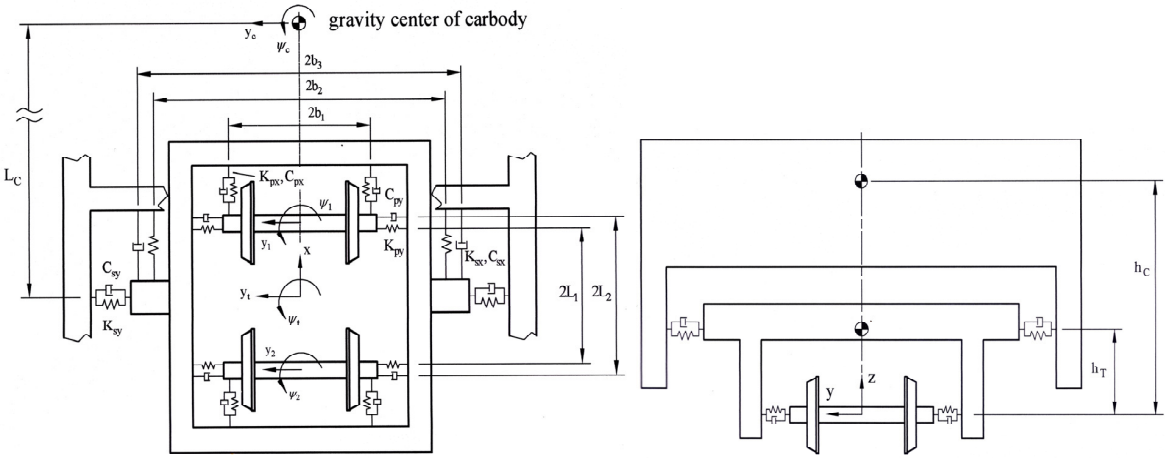

(a) (b)

Fig. 1. Car body model. (a) Top view and (b) Front view.

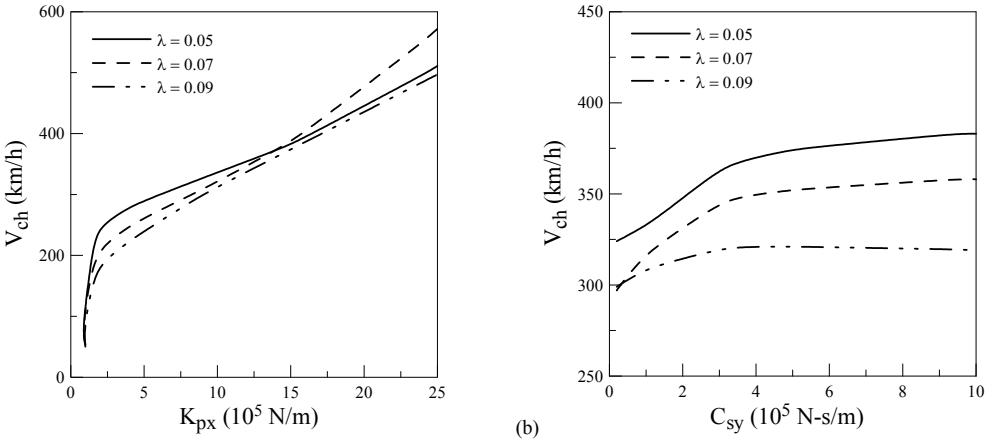

Fig. 2. Effect of (a) longitudinal stiffness of primary suspension and (b) lateral damping of secondary suspension on critical hunting speeds with various wheel conicities.

References

[1] H. Molatefi, M. Hecht, M. H. Kadivar, Effect of Suspension System in the Lateral Stability of Railway Freight Trucks, Proceedings of the Institution of Mechanical Engineers, Part F: Journal of Rail and Rapid Transit 221(3) (2007) 399-407.

[2] O. Polach, A Fast Wheel-Rail Forces Calculation Computer Code, Vehicle System Dynamic 33(Suppl) (1999) 728-739.

[3] Y.Z. Liang, K.T. Fang, Q.S. Xu, Uniform Design and its Applications in Chemistry and Chemical Engineering, Chemometrics and intelligent Laboratory Systems 58 (2001) 43-57.

[4] L. Peng, Y.Z. Wang, G.M. Dai, Z.S. Cao, A Novel Differential Evolution with Uniform Design for Continuous Global Optimization, Journal of Computers 7(1) (2012) 3-10.

[5] Y.Z. Yang, M. Jiang, J. Xu, Y.H. Ma, J. Tong, Uniform Design of Optimizing Formulation of Friction Materials with Composite Mineral Fiber (CMF) and their Friction and Wear Behavior, Applied Composite Materials 19(2) (2012) 161-170.

[6] J.F. Kennedy, R.C. Eberhart, Particle Swarm Optimization, Proceedings of IEEE International Conference on Neural Networks (1995) 1942-1948.

[7] F. Van Den Bergh, A.P. Engelbrecht, A Cooperative Approach to Particle Swarm Optimization, IEEE Transactions on Evolutionary Computation 8(3) (2004) 225-239.

[8] J. Sun, B. Feng, W. Xu, Particle Swarm Optimization with Particles Having Quantum Behavior, IEEE Congress on Evolutionary Computation 2 (2004) 325-331.

[9] J. Sun, B. Feng, W. Xu, 2004. A Global Search Strategy of Quantum-Behaved Particle Swarm Optimization, IEEE Conference on Cybernetics and Intelligent Systems (2004) 111-116.

[10] Y.C. Cheng, Hunting Stability Analysis of a Railway Vehicle System using a Novel Non-linear Creep Model, Proceedings of the Institution of Mechanical Engineers, Part F: Journal of Rail and Rapid Transit 226(6) (2004) 612-629.

[11] V.K. Garg, R.V. Dukkipati, Dynamics of Railway Vehicle Systems, Academic Press, Canada, 1984.

[12] D. Horak, , D.N. Wormley, Nonlinear Stability and Tracking of Rail Passenger Trucks, Transactions of the ASME, Journal of Dynamic Systems, Measurement, and Control 104(3) (1982) 256-263.

[13] M. Vidyasager, Nonlinear Systems Analysis, Prentice-Hall Press, 1978.

[14] A.K.W. Ahmed, S. Sankar, Lateral Stability Behavior of Railway Freight Car System with Elasto-Damper Coupled Wheelset: Part 2 - Truck Model, Transactions of the ASME, Journal of Mechanisms, Transmissions, and Automation in Design 109(4) (1987) 500-507.

[15] Y. Wang, K.T. Fang, A Note on Uniform Distribution and Experimental Design, Kexue Tongbao 26(6) (1981) 485-489.